THE JOURNAL OF BIOLOGICAL CHEMISTRY
Vol. 273, No. 17, Issue of April 24, pp. 10445–10453, 1998

Printed in U.S.A.

Functional Microdomains in G-protein-coupled Receptors

THE CONSERVED ARGININE-CAGE MOTIF IN THE GONADOTROPIN-RELEASING HORMONE RECEPTOR*

(Received for publication, November 13, 1997, and in revised form, February 2, 1998)

Juan Ballesteros‡§, Smiljka Kitanovic§¶, Frank Guarnieri‡‖, Peter Davies, Bernard J. Fromme**, Karel Konvicka‡, Ling Chi¶, Robert P. Millar**, James S. Davidson**, Harel Weinstein‡, and Stuart C. Sealfon¶‡‡§§**

*From the ‡Department of Physiology and Biophysics, ¶Fishberg Research Center in Neurobiology, and ‡‡Department of Neurology, Mount Sinai School of Medicine, New York, New York 10029 and **Department of Chemical Pathology, University of Cape Town, Observatory 7925, Cape Town, South Africa*

An Arg present in the third transmembrane domain of all rhodopsin-like G-protein-coupled receptors is required for efficient signal transduction. Mutation of this Arg in the gonadotropin-releasing hormone receptor to Gln, His, or Lys abolished or severely impaired agonist-stimulated inositol phosphate generation, consistent with Arg having a role in receptor activation. To investigate the contribution of the surrounding structural domain in the actions of the conserved Arg, an integrated microdomain modeling and mutagenesis approach has been utilized. Two conserved residues that constrain the Arg side chain to a limited number of conformations have been identified. In the inactive wild-type receptor, the Arg side chain is proposed to form an ionic interaction with $Asp^{3.49(138)}$. Experimental results for the $Asp^{3.49(138)} \rightarrow$ Asn mutant receptor show a modestly enhanced receptor efficiency, consistent with the hypothesis that weakening the $Asp^{3.49(138)}$-$Arg^{3.50(139)}$ interaction by protonation of the Asp or by the mutation to Asn favors activation. With activation, the $Asp^{3.49(138)}$-$Arg^{3.50(139)}$ ionic bond would break, and the unrestrained Arg would be prevented from orienting itself toward the water phase by a steric clash with $Ile^{3.54(143)}$. The mutation $Ile^{3.54(143)} \rightarrow$ Ala, which eliminates this clash in simulations, causes a marked reduction in measured receptor signaling efficiency, implying that solvation of $Arg^{3.50(139)}$ prevents it from functioning in the activation of the receptor. These data are consistent with residues $Asp^{3.49(138)}$ and $Ile^{3.54(143)}$ forming a structural motif, which helps position Arg in its appropriate inactive and active receptor conformations.

The gonadotropin-releasing hormone (GnRH)[1] receptor is a member of the rhodopsin-like G-protein-coupled receptor (GPCR) family (1, 2). These heptahelical proteins include the visual opsins and various receptors for neurotransmitters, peptides, and glycoproteins. Activation of these receptors by their diverse agonists is associated with conformational changes in the receptor that facilitate a signal-propagating interaction with G-proteins (3). These conformational changes can involve relative movement of helices, as reported for rhodopsin (4, 5) and/or rotation of the helices as found in a constitutively active adrenergic receptor (6).

Sequence alignment of GPCRs shows that certain amino acids are highly conserved at corresponding positions within the putative transmembrane domains (TMD) (7). Transitions among receptor conformations may reflect dynamic changes in side chain interactions within the receptor. Two of these conserved residues have been studied by reciprocal mutation in the GnRH and serotonin receptors, and the results suggest that the TMD 2 and 7 side chains have an interdependent role in receptor activation (8, 9). Most likely several other conserved side chains also interact to form the skeleton required for the conformational rearrangements that accompany the transition between inactive and active receptor states.

The elucidation of the intramolecular interactions and conformational changes underlying receptor activation is hindered by the absence of high resolution structural data for any GPCR. The available low resolution projection maps of rhodopsin do not allow inferences about specific side chain interactions (10, 11). A prevalent approach to investigate structure-function relations of GPCRs is to introduce structural perturbations via site-directed mutagenesis and to evaluate their effect on receptor phenotype in binding and signal transduction assays (12). However, determining the phenotype of mutant receptors does not lead to an unequivocal interpretation concerning the structural basis of that phenotype (13).

Molecular modeling has facilitated the integration of experimental observations and biophysical data into a mechanistic scheme for receptor structure and function (12, 14). Structural and functional details of ligand binding (15, 16) and receptor activation by agonist complexing (8, 17) and by constitutively activating mutations (18) have been simulated in such models. The receptor models can thus provide a rationalization of current experimental data within a structural framework in which to explore the mechanisms underlying the functional perturbations induced by activation. However, caveats concerning the computational approaches arise from the complexity of these structures and the relative paucity of pertinent experimental data at atomic detail. Not surprisingly, given a limited number of experimentally determined constraints, the proposed models may exhibit inconsistent interaction patterns. In addition, GPCR models usually are not studied in the appropriate aqueous/membrane interface environment, making it less likely that the key side chain interactions are modeled accurately, especially those involving side chains near or separated by this interface.

* This work was supported by National Institutes of Health Grants RO1 DK46943, 5T32DA07135, and KO5 DA00060. The costs of publication of this article were defrayed in part by the payment of page charges. This article must therefore be hereby marked "*advertisement*" in accordance with 18 U.S.C. Section 1734 solely to indicate this fact.

§ The first two authors contributed equally to this work.
‖ Present address: Sarnoff Corp., 201 Washington Rd., Princeton, NJ 08543.
§§ Fishberg Center for Neurobiology Research, Box 1065, Mount Sinai School of Medicine, One Gustave Levy Place New York, NY 10029. Tel.: 212-241-7075; Fax: 212-996-9785; E-mail: sealfon@msvax.mssm.edu.

[1] The abbreviations used are: GnRH, gonadotropin-releasing hormone; GPCR, G-protein-coupled receptor; TMD, transmembrane domain.

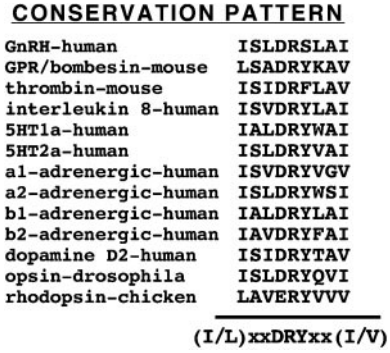

FIG. 1. **The conservation pattern of the cytoplasmic side of TMD 3 is demonstrated in an alignment of several GPCRs.**

To overcome the limitations inherent in both site-directed mutagenesis and computational modeling, we have integrated mutational studies and the application of computational techniques to the study of structural motifs in the receptor that may constitute functional microdomains. The inferences from studies of these microdomains, whose proposed structure can be substantiated by experimental data, are then evaluated in the context of a whole receptor model. This approach facilitates the elucidation of a structural basis for the phenotypes induced by site-directed mutagenesis. The effect of mutations is tested first in the microdomain models and correlated with the functional effects of site-directed mutant receptors expressed in mammalian cells. Using this approach, we have recently mapped precise interactions in segments of the binding pocket of the serotonin $5HT_{2A}$ receptor (19).

In the present report, we have applied this approach to study the interaction pattern of the conserved Arg in TMD 3 in the GnRH receptor. The conserved arginine $Arg^{3.50}$ (see "Experimental Procedures" for locus numbering scheme) has been implicated in the activation of various GPCRs by mutagenesis studies (20, 21) and by computational modeling (21, 22). An understanding of the molecular basis for the functional role of this Arg requires identification of those residues whose specific interactions determine its orientation within the structure of the receptor. Given the great conformational flexibility of the Arg side chain, it is likely that such orienting residues would form a three-dimensional motif to which we refer as the arginine cage.

Specific partners for $Arg^{3.50}$ have been proposed, such as the conserved Asp in TMD 2 ($Asp^{2.50}$) (21, 22), based on the rationale of a similar conservation pattern and the need to neutralize a positive charge in a low dielectric environment. However, a complete exploration of the conformational space of $Arg^{3.50}$ in the context of a full molecular model of the receptor is not attainable with present computational techniques, and several other candidate interacting residues can be proposed. In particular, analysis of the conservation pattern centered on $Arg^{3.50}$ identifies highly conserved residues that could influence the conformation of $Arg^{3.50}$. These residues form the consensus sequence (I/L)*XX*DRY*XX*(I/V) (Fig. 1). $Arg^{3.50}$, $Asp/Glu^{3.49}$, and $Ile/Val^{3.54}$ are present in all cloned GPCRs belonging to the rhodopsin family, with the exception of the platelet-activating factor receptor, which has an asparagine residue at position 3.49 (23). In an α-helical environment, the conservation pattern described above forms an envelope of conserved residues surrounding $Arg^{3.50}$, consisting in the GnRH receptor of $Ile^{3.46(135)}$, $Asp^{3.49(138)}$, and $Ile^{3.54(143)}$ (Fig. 2).

To evaluate the role of these various conserved residues in caging the $Arg^{3.50}$ side chain in the inactive and active forms of the receptor, we have performed a complete conformational exploration of TMD 3 using Monte Carlo simulations (15). The helical structure and the helix ends of TMD 3 have been experimentally substantiated by Cys scanning of the D2 receptor (24) and by spin-labeling studies of rhodopsin, in which the membrane/aqueous interface has been located between residues 3.52 and 3.53 (25). For the Monte Carlo simulations, a novel biphasic solvent model has been developed that reproduces the interface between the interior of a protein and a water environment.[2] Using this Monte Carlo approach, the inferences about the possible caging interactions involving the conserved Arg have been tested by evaluating computationally the structural effects of mutations in this TMD 3 domain model and correlating these results with the functional effects of site-directed mutagenesis. These studies provide insight into the role of $Arg^{3.50(139)}$ in sustaining a pattern of interactions that may occur in the active and inactive forms of the receptor.

EXPERIMENTAL PROCEDURES

Residue Numbering Scheme—The residues in TMDs are numbered relative to the most conserved residue contained in the helix, as explained previously (14). On the basis of this scheme, the most conserved residue in TMD 3, Arg-139, is designated with the index number 3.50 and is hence referred to throughout as $Arg^{3.50(139)}$; the identification of the preceding Asp is $Asp^{3.49(138)}$.

Computational Methods—The segment of TMD 3 from $Cys^{3.25}$ to $Thr^{3.55}$ was modeled as an α-helix. These helix boundaries, predicted following methodology described elsewhere (14), are consistent with recent experimental results for other GPCRs (24, 25). The environment surrounding the Arg residue in TMD 3 has been investigated in rhodopsin and found to consist of two distinct phases: a water phase and a membrane-embedded helix (25). The environment of $Arg^{3.50(139)}$ in the helix was assumed to be similar to the environment of residues buried inside the protein interior, consonant with studies on the known structure of the photosynthetic reaction center (26), and has been modeled by a distance-dependent dielectric. To simulate the biphasic environment in our calculations, the novel mixed solvent model includes a water phase and a distance-dependent dielectric phase.[2] The boundary between the two phases consists of a plane parallel to the membrane. TMD 3 was initially positioned perpendicular to the membrane plane at the midpoint between residues 3.52 and 3.53 following experimental observations (23) but was allowed to move $\pm$ 2.3 Å vertically in the direction normal to the membrane plane to prevent arbitrary effects arising from the initial positioning.

To explore the conformational space available for the cytoplasmic portion of helix 3, Monte Carlo simulations were performed by varying the torsional angles for residues $Val^{3.44(133)}$ to $Thr^{3.55(144)}$. The variation of backbone dihedral angles ϕ and ψ were restrained to $\pm$ 20° from their initial values. Side chain dihedral angles were rotated freely. Extensive simulations are necessary to reach convergence of the resulting conformations described by the rotamers we analyzed (see below for a description of the four consecutive dihedral angles defining the rotamers). Thus, between 100 and 400 rounds of independent random simulations were performed for each TMD 3 construct. In each round, repeated runs of Monte Carlo-simulated annealing were performed from a starting temperature of T_1 = 2070 K, with a cooling schedule of $T_{n+1} = 0.9 \times T_n$ and 10,000 steps per temperature to reach 310 K. Between 19 and 76 million conformations were thus sampled for each wild-type and mutant construct. Analysis of the resulting conformations was performed at T = 310 K and restricted to backbone conformations within $\pm$ 10° from their initial values to maintain an α-helical conformation.

The conformations of the side chains, in particular the $Arg^{3.50(139)}$ side chain, are defined by the corresponding dihedral angles $\chi 1$, $\chi 2$, $\chi 3$, $\chi 4$. These dihedral angles are classified according to three main rotamers: gauche plus (g+) centered on −60° (encompassing angle values between −120° and 0°), gauche minus (g−) centered on +60° (between 0° and 120°), and trans (t) centered on 180° (between 120° and −120°). Evaluation of the preferred conformations was performed by analyzing the populations of each side chain rotamer. The rotamer state of the Arg side chain is defined by the state of each one of its four dihedral angles, *e.g.* the propensity of each dihedral angle ($\chi 1$, $\chi 2$, $\chi 3$, $\chi 4$) to adopt the (g+, g−, t) configuration. There are 81 possible Arg side chain rotamers, which were grouped according to their spatial orientation toward specific residues in TMD 3. The spatial orientation of each $Arg^{3.50(139)}$ rotamer was inferred from the average values of each of the four

[2] F. Guarnieri, manuscript in preparation.

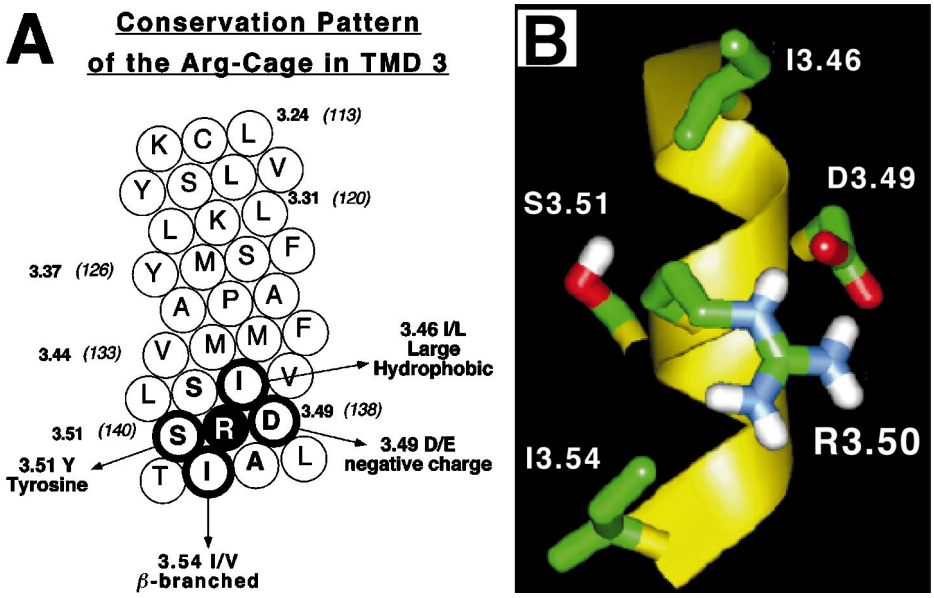

FIG. 2. **Spatial proximity between the conserved Arg$^{3.50(139)}$) and the conserved residues surrounding it in TMD 3.** *A*, helical net of TMD 3 of the human GnRH receptor showing Arg$^{3.50(139)}$ surrounded by conserved residues. *B*, three-dimensional computational model of TMD 3 of the GnRH receptor showing the spatial proximity of the conserved residues surrounding the Arg residue.

dihedrals defining each rotamer.

The Arg-cage microdomain resulting from this conformational analysis was positioned in the context of a complete model of the transmembrane helix bundle of the GnRH receptor (9), constructed to follow the electron microscopy projection map of rhodopsin (10) using methodological steps and approaches described in detail elsewhere (14).

DNA Constructs and Transfection—Procedures for site-directed mutagenesis of the GnRH receptor, subcloning of the receptor coding region into pcDNA1/Amp and transient receptor expression have been described previously (27). COS-1 cells transfected with plasmid DNA were maintained in Dulbecco's modified Eagle's medium containing 10% fetal bovine serum. One day after transfection, COS-1 cells were split from 100-mm plates into two 12-well plates for the functional assay or into two 24-well plates for the whole-cell binding assay. Mutations of Asp$^{3.49(138)}$ and Arg$^{3.50(139)}$ were done in the mouse GnRH receptor, whereas mutations of Ile$^{3.46(135)}$ and Ile$^{3.54(143)}$ were generated in the human GnRH receptor.

Binding and Functional Assays—Binding of GnRH to the wild-type and mutant receptors was measured at 4 °C in a whole-cell agonist competition binding assay 72 h after transfection (13). ^{125}I-GnRH-A ((des-Gly^{10}, D-Ala^{6}, GnRH-ethylamide) was used as the label and displaced by increasing concentrations of GnRH. The K_d for GnRH-A was estimated from homologous competition binding. The radioactivity bound to membranes or cells was counted in a γ-counter, and the amount of protein per well was determined using the Lowry method (28). The phosphatidylinositol hydrolysis assay was performed as described earlier (27). The binding and concentration-response curves were fitted using Kaleidagraph software (27). K_i and B_{max} values were determined by using the program LIGAND (29).

Receptor Efficiency—We have developed an empirical representation for receptor efficiency (Q) using operational models of occupancy and response (see Equations 1 and 2),

$$[AR]/B_{max} = 1/(1 + K_d/[A]) \quad \text{(Eq. 1)}$$

$$E/E_{max} = 1/(1 + EC_{50}/[A]) \quad \text{(Eq. 2)}$$

where [AR] represents the concentration of ligand-receptor complex, [A] is the concentration of free ligand, and E_{max} and B_{max} represent the maximal response and maximal binding, respectively. Receptor efficiency (Q) represents the quantal functional response achieved per agonist-occupied receptor. To allow comparison of the various mutant receptors and to accommodate the influence of spare receptors on EC_{50} values (27), we define receptor efficiency as (see Equation 3),

$$Q = E/[AR] \quad \text{(Eq. 3)}$$

E represents the functional response obtained at a concentration of occupied receptor [AR] in the presence of agonist concentration [A] corresponding to the EC_{50} value for that particular receptor and agonist. For the GnRH receptor constructs, the agonist utilized for calculating Q is GnRH. Substituting and solving for Q, where [A] = EC_{50}, gives (see Equation 4)

$$Q = (1/2) \times [(K_d + EC_{50})/EC_{50}] \times (E_{max}/B_{max}) \quad \text{(Eq. 4)}$$

In calculating Q, K_i has been used as an estimate of K_d. The receptor efficiency values obtained for the various receptor constructs are expressed relative to the wild-type receptor value.

RESULTS

Computational Simulations of TMD 3 Segment Surrounding Arg$^{3.50(139)}$

The GPCRs demonstrate a pattern of conservation among several residues that are in spatial proximity to Arg$^{3.50(139)}$ when the cytoplasmic side of TMD 3 is modeled as a regular α-helix (see Fig. 2). These potential local sites of interaction for Arg$^{3.50}$ include the large hydrophobic residue (Ile/Val/Leu) at position 3.46, the acidic residue at position 3.49, the Tyr (Ser in the GnRH receptor) at position 3.51, and the β-branched large hydrophobic residue (Ile/Val) at position 3.54.

The interaction patterns and rotamer positioning of Arg$^{3.50(139)}$ with respect to these neighboring TMD 3 residues were explored with Monte Carlo simulations for the wild-type helix and for various mutant receptors. Many conformations of the flexible Arg side chain were not attainable due to steric clashes with the helix backbone. For example, all Arg rotamers whose $\chi 1 = g-$ are unpopulated because of a clash between the Arg γ-methyl and the backbone carbonyl from the preceding turn of the helix (30).

The most striking observation to emerge from the simulations is the tendency for Arg$^{3.50(159)}$ to form an ionic bond with Asp$^{3.49(138)}$, as illustrated in Fig. 2*B*. Nearly half of the Arg$^{3.50(139)}$ rotamers observed were bound to this aspartic acid (Table I). As shown in Fig. 3, a variety of Arg conformations were identified that form the Arg-Asp interaction. Most other side chains remained in their original orientations throughout the simulations, consistent with their preferred rotamer populations in known α-helical structures. Ser and Thr residues were overwhelmingly (92–99% of rotamers) in the $\chi 1 = g+$ conformation due to H-bonding to the backbone carbonyl of the preceding turn (30, 31). β-Branched residues (Val, Ile, Thr), except Ile$^{3.54(143)}$, were constrained to one single $\chi 1$ population (83–99% of rotamers) due to clashes with the helix backbone (30). The structural effects of several mutations of the residues surrounding Arg$^{3.50(139)}$ were studied computationally:

Ile$^{3.46(135)}$—The side chain at this position is not as well conserved as the other residues surrounding Arg$^{3.50}$. Although Ile is most commonly found at this site, Leu or Met also occur

TABLE I

Preferred conformations of the $Arg^{3.50(139)}$ side chain-based rotamer populations for the wild-type and $Asp^{3.49(138)}$-modified receptor by mutation ($Asp^{3.49(138)} \rightarrow Asn$) or protonation ($Asp^{3.49(138)} \rightarrow Asp$-H)

Orientation indicates the side chain locus that is in proximity to the $Arg^{3.50(139)}$ head group. All listed values are expressed as the percentage of total rotamer populations observed for each construct. Only rotamer populations present at greater than 5% for at least one of the constructs are shown.

Orientation of $Arg^{3.50}$ side chain	Mode of stabilization	Dihedral angles of $Arg^{3.50}$ side chain				Rotamer populations		
		$\chi1$	$\chi2$	$\chi3$	$\chi4$	Wild type	$Asp^{3.49}$Asn	$Asp^{3.49}$Asn-H
Locus 3.49	salt bridge	g+	g+	g−	t	11.9	0.0	0.0
Locus 3.49	salt bridge	g+	g−	t	t	11.1	0.0	1.0
Locus 3.49	salt bridge	t	g−	g+	g−	6.3	2.8	0.0
Locus 3.49	salt bridge	t	g−	g−	g+	7.9	0.0	5.1
Locus 3.49	salt bridge	t	g−	g−	t	8.3	0.1	6.5
Total rotamer populations with side chain of residue $Arg^{3.50}$ oriented toward locus 3.49						45.5	2.9	12.6
Locus 3.51	H-bond	t	t	g−	g+	0.5	7.0	5.9
Locus 3.51	H-bond	t	t	t	g+	0.0	3.2	11.6
Locus 3.51	H-bond	t	t	g−	t	0.0	12.9	10.3
Locus 3.51	H-bond	t	t	g−	g−	0.0	14.0	13.8
Total rotamer populations with side chain of residue $Arg^{3.50}$ oriented toward locus 3.51						0.5	37.1	41.6
Locus 3.54	H_2O solvation	t	g−	t	g+	0.0	7.5	0.5
Locus 3.54	H_2O solvation	t	g−	t	t	3.2	21.0	6.6
Locus 3.54	H_2O solvation	t	g−	t	g−	0.9	0.9	5.8
Total rotamer populations with side chain of residue $Arg^{3.50}$ oriented toward locus 3.54						4.1	29.4	12.9

in different receptors. For the simulations, we substituted $Ile^{3.46(135)}$ with Ala, Val, and Leu to test 1) the functional relevance of the wild-type side chain (by substituting Ala), 2) the role of the β-branched character of the residue (by substituting Val), and 3) the effect of the large hydrophobic side chain (by substituting Leu). Monte Carlo simulations of all three mutant constructs showed that the conformational preferences of the Arg side chain were similar to those found in the wild-type receptor. Therefore, according to our results, $Ile^{3.46(135)}$ does not modulate the orientation of $Arg^{3.50(139)}$.

$Asp^{3.49(138)}$—Monte Carlo simulations were performed for a mutation of the conserved acidic residue to Asn. By neutralizing the charge at this locus, this $Asp^{3.49(138)} \rightarrow$ Asn mutant would weaken the ionic bond between $Arg^{3.50(139)}$ and $Asp^{3.49(138)}$ observed in simulations of the wild-type receptor. This mutation was found to significantly affect the conformational preferences of the Arg side chain (see Table I). In the $Asp^{3.49(138)} \rightarrow$ Asn mutant, the Arg side chain rarely interacts with the 3.49 locus (3% of rotamers). Two new orientations appear populated, as shown in Fig. 4. 1) $Arg^{3.50(139)}$ is oriented toward positions 3.47–3.51 where it can H-bond to $Ser^{3.47(136)}$ and $Ser^{3.51(140)}$ (37% of rotamers). 2) $Arg^{3.50(139)}$ is oriented toward positions 3.53–3.54 where it can be solvated by water at the cytoplasmic boundaries. Because activation of rhodopsin has been shown to involve a proton uptake by $Glu^{3.49}$ (32, 33), simulations were also performed for the protonated form of the aspartic acid, termed $Asp^{3.49(138)} \rightarrow$ Asp-H. The results yielded a pattern of preferred conformations very similar to that of $Asp^{3.49(138)} \rightarrow$ Asn (Table II).

$Ser^{3.51(140)}$—A Tyr residue most commonly occurs at this position in other GPCRs. We tested the functional role of this residue with the mutant construct $Ser^{3.51(140)} \rightarrow$ Ala. Hydrogen-bonding between $Arg^{3.50(139)}$ and $Ser^{3.51(140)}$ was observed in the $Asp^{3.49(138)} \rightarrow$ Asn mutant receptor, but the mutation $Ser^{3.51(140)} \rightarrow$ Ala did not change significantly the orientation of the Arg side chain relative to the wild-type construct (data not shown). Evidently, this H-bond is not energetically competitive with the ionic bond $Arg^{3.50(139)}$-$Asp^{3.49(138)}$.

$Ile^{3.54(143)}$—Only Ile or Val residues appear in GPCR sequences at this position. Therefore, this locus always contains a bulky β-branched, hydrophobic side chain. To test the structural implications of these properties, we substituted this residue by Val, Leu, and Ala. The Val side chain displays similar structural features as isoleucine, being hydrophobic, bulky, and β-branched. Leu is hydrophobic and bulky but has a γ-branched side chain. Ala is hydrophobic but neither bulky nor branched. Analysis of all rotamers populated over 5%, shown in Table II, indicates that the prevailing interaction for the wild-type receptor and the three mutants is still the ionic bond between $Arg^{3.50(139)}$ and $Asp^{3.49(138)}$ (65–80% of rotamers). Although maintaining the same interaction, the individual rotamer conformations preferred for this interaction vary among the mutants and with respect to the wild-type receptor (Table II). Of note, a novel orientation for the Arg side chain toward residues 3.53–3.54 appears significantly populated in the $Ile^{3.54(143)} \rightarrow$ Ala mutant (14.3%) but not in the wild-type, $Ile^{3.54(143)} \rightarrow$ Val, or $Ile^{3.54(143)} \rightarrow$ Leu mutants. In the $Ile^{3.54(143)} \rightarrow$ Ala mutant, the Arg side chain can be positioned toward the aqueous cytoplasm, as illustrated in Fig. 5.

Radioligand Binding and Agonist-stimulated Inositol Phosphate Accumulation by the Wild-type and Mutant Receptors—To correlate the predicted local structural roles of the conserved TMD 3 residues with their effect on receptor function, constructs obtained from the mutation of $Arg^{3.50(139)}$ and its surrounding conserved residues (see Fig. 2) were tested for their effects on ligand binding and inositol phosphate accumulation (Table III). The mutation of the $Asp^{3.49(138)}$, $Arg^{3.50(139)}$, and $Ser^{3.51(140)}$ loci were carried out on the mouse GnRH receptor, whereas the $Ile^{3.46(135)}$ and $Ile^{3.54(143)}$ mutants were generated in the human GnRH receptor. Both human and mouse GnRH receptors have identical sequences in the TMD 3 segment studied. The amino acid substitutions were designed to test the side chain property conserved at each locus and/or a specific functional hypothesis derived from the modeling studies. The results of the radioligand binding and phosphatidylinositol assay and the relative coupling efficiencies of the various receptor constructs are summarized in Table III.

$Ile^{3.46(135)}$—Removal of the Ile side chain by the $Ile^{3.46(135)} \rightarrow$ Ala mutation abolished binding and activation. Substitution by another β-branched residue $Ile^{3.46(135)} \rightarrow$ Val also eliminated detectable ligand binding and signal transduction. In contrast, the $Ile^{3.46(135)} \rightarrow$ Leu receptor manifested coupling comparable

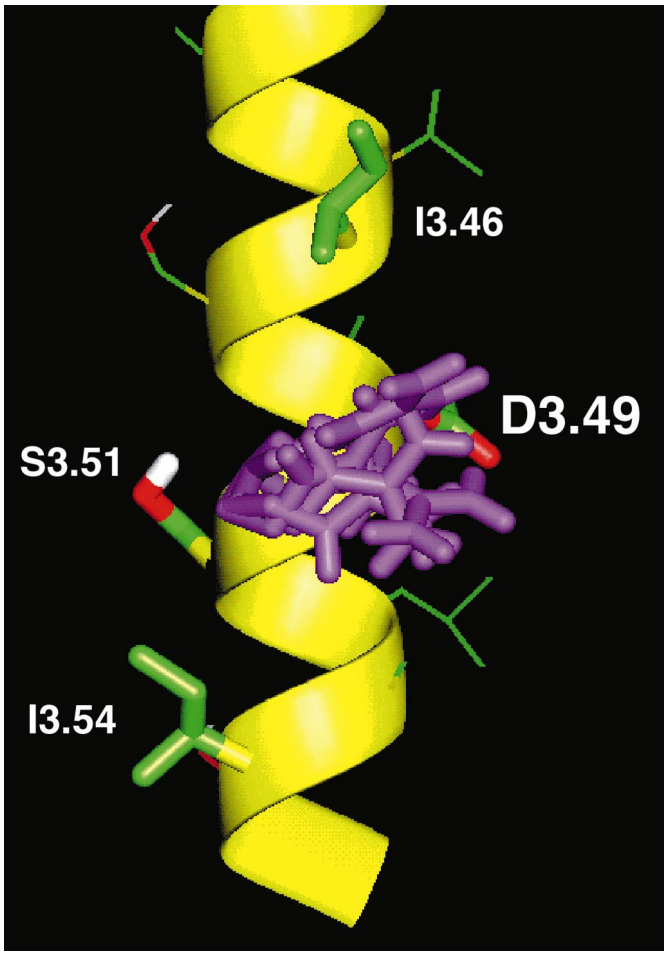

FIG. 3. **Wild-type $R^{3.50(139)}$ orientations.** Three-dimensional model of TMD 3 of the GnRH receptor illustrating the preferred conformations of the Arg side chain (*purple*) in the wild-type construct. Conserved residues are highlighted by *thicker bonds*. Note that all populated rotamer conformations are oriented toward $Asp^{3.49(138)}$, driven by an ionic bond between $Arg^{3.50(139)}$ and $Asp^{3.49(138)}$.

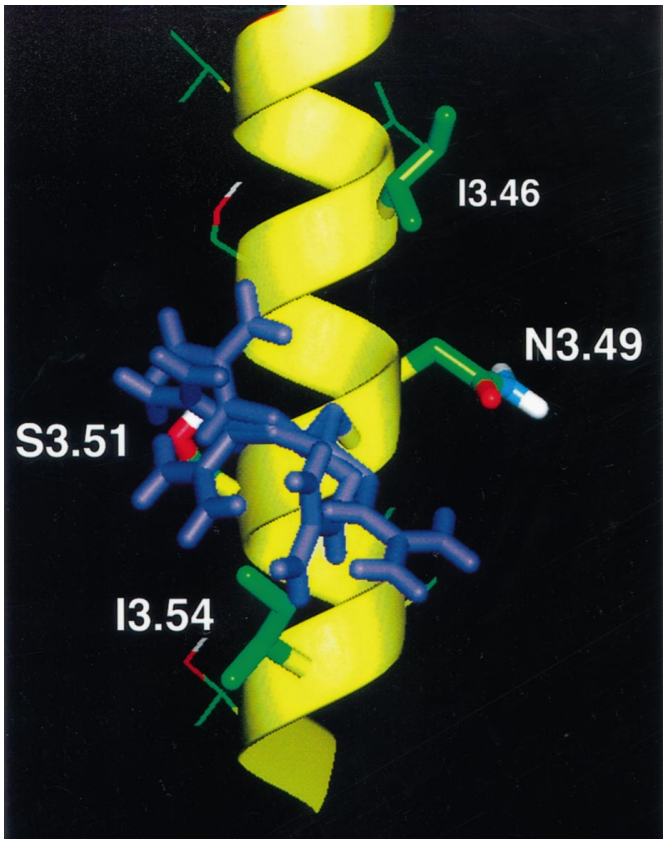

FIG. 4. **$Arg^{3.50(139)}$ orientations in the $D^{3.49(138)}N$ mutant.** Three-dimensional model of TMD 3 of the GnRH receptor illustrating the preferred conformations of the Arg side chain (*purple*) in the $D^{3.49(138)}N$ construct. Conserved residues are highlighted by *thicker bonds*. Note that all the populated rotamer conformations are oriented away from $Asn^{3.49(138)}$. Instead, $Arg^{3.50(139)}$ is oriented either toward $Ser^{3.51(140)}$-$Ser^{3.47(136)}$ (37.1%), where it can H-bond to the Ser residues, or toward the cytoplasm at the level of $Ile^{3.54(143)}$-$Ala^{3.53(142)}$ (29.4%), where it would be solvated.

to that of the wild-type receptor. However, due to poor expression of the $Ile^{3.46(135)} \rightarrow$ Leu receptor (13% of wild-type receptor B_{max}), the calculated value for receptor efficiency for this mutant reveals a 5-fold increase above the value obtained for the wild-type receptor (Table III). The affinity of this mutant construct for GnRH is comparable to the wild-type receptor. The restricted pattern of amino acid substitutions that are functionally tolerated at the 3.46(135) position is most consistent with this site being involved in helix-helix packing (see "Discussion").

$Asp^{3.49(138)}$—The $Asp^{3.49(138)} \rightarrow$ Ala mutant had no detectable agonist binding or activation and could not be evaluated. The more conservative mutation $Asp^{3.49(138)} \rightarrow$ Asn behaved like wild type in terms of its K_i, EC_{50}, and E_{max} values (Table III). However, the lower B_{max} (56% relative to wild type) suggests that this construct has a modestly enhanced signaling efficiency.

$Arg^{3.50(139)}$—Mutations of $Arg^{3.50(139)}$ to His and Lys yielded constructs with no detectable binding or activation. The $Arg^{3.50(139)} \rightarrow$ Gln mutant expressed well and had wild-type affinity for GnRH but was very poorly coupled (Table III).

$Ser^{3.51(140)}$—Consistent with the lack of structural effects observed with mutation of this locus in the computational simulations, the phenotype of the expressed $Ser^{3.51(140)} \rightarrow$ Ala mutant receptor was similar to that of the wild-type receptor (data not shown). This finding is consistent with results reported previously (34).

$Ile^{3.54(143)}$—The effects of mutating this locus to Val, Leu, and Ala were examined. In comparison with the wild-type receptor, the affinity of GnRH was modestly decreased for the Ala-substituted receptor. The $Ile^{3.54(143)} \rightarrow$ Ala receptor showed a marked reduction in signaling efficiency, whereas the substitutions with Leu or Val were well tolerated (Table III).

DISCUSSION

$Arg^{3.50}$ is absolutely conserved in all GPCRs, and its substitution in various GPCRs severely affects signal transduction (20, 21). The pattern of conservation and the effects of mutations make it likely that this side chain serves a key role in conformational changes and interactions underlying receptor activation. The results obtained with mutation of this locus in the GnRH receptor support a crucial role for this Arg in receptor function. Among the mutant receptors studied, only the construct with a Gln substitution at this site shows any detectable signal transduction. Similar results obtained by mutating the $Arg^{3.50}$ in the mouse GnRH receptor have been recently reported (34).

Oliveira *et al.* (22) proposed a mechanism for receptor activation in which the change in orientation of this $Arg^{3.50}$ constitutes an Arg-switch leading to activation of GPCRs, a hypothesis recently expanded by a combination of mutagenesis and computational simulations on adrenergic receptors (21, 35). The present study has focused on the molecular details of the microdomains surrounding $Arg^{3.50}$ by delineating the neighboring residues that interact with or restrict the position-

TABLE II

Preferred conformations of the Arg$^{3.50(139)}$ side chain based on rotamer populations for the wild-type and Ile$^{3.54(143)}$ mutants to Ala, Leu, and Val

All listed values are expressed as the percentage of total rotamer populations observed for each construct. Only rotamer populations greater than 5% for at least one of the constructs are shown.

Orientation of Arg$^{3.50}$ side chain	Mode of stabilization	Dihedral angles of Arg$^{3.50}$ side chain				Rotamer populations			
		χ1	χ2	χ3	χ4	Wild type	Ile$^{3.54}$Ala	Ile$^{3.54}$Leu	Ile$^{3.54}$Val
Locus 3.49	salt bridge	g+	g+	g+	t	2.9	6.8	4.1	6.3
Locus 3.49	salt bridge	g+	g+	t	g+	3.6	18.9	7.3	3.3
Locus 3.49	salt bridge	g+	g+	t	t	3.5	9.9	7.6	5.6
Locus 3.49	salt bridge	g+	g+	g−	t	11.9	2.8	4.7	3.2
Locus 3.49	salt bridge	g+	g−	g+	t	1.4	0.0	6.9	0.5
Locus 3.49	salt bridge	g+	g−	t	t	11.1	5.8	3.3	5.5
Locus 3.49	salt bridge	g+	g−	t	g−	0.2	0.5	5.2	1.2
Locus 3.49	salt bridge	t	g−	g+	g+	3.8	2.3	4.2	6.7
Locus 3.49	salt bridge	t	g−	g+	t	4.3	0.9	8.4	6.5
Locus 3.49	salt bridge	t	g−	g+	g−	6.3	3.1	5.5	4.5
Locus 3.49	salt bridge	t	g−	g−	g+	7.9	12.5	19.5	15.5
Locus 3.49	salt bridge	t	g−	g−	t	8.3	3.0	3.7	16.4
Total rotamer populations with side chain of residue Arg$^{3.50}$ oriented toward locus 3.49						65.2	66.5	80.4	75.2
Locus 3.54	H_2O solvation	t	g−	t	g+	0.0	12.7	0.0	0.0
Locus 3.54	H_2O solvation	t	g−	t	t	3.2	1.6	3.1	5.3
Total rotamer populations with side chain of residue Arg$^{3.50}$ oriented toward locus 3.54						3.2	14.3	3.1	5.3

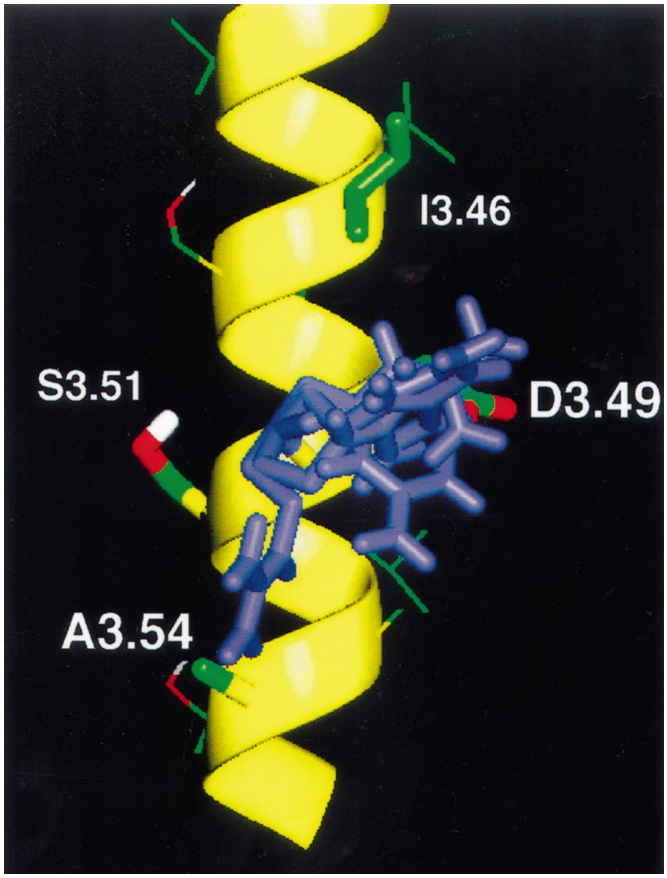

FIG. 5. **R$^{3.50(139)}$ orientations in the I$^{3.54(143)}$A construct.** Three-dimensional model of TMD 3 of the GnRH receptor illustrating the preferred conformations of the Arg side chain (*purple*) in the Ile$^{3.54(143)}$ → Ala construct. Conserved residues are highlighted by *thicker bonds*. Most of the populated rotamer conformations are oriented toward Asp$^{3.49(138)}$, as observed for the wild-type (Fig. 4), driven by an ionic bond between Arg$^{3.50(139)}$ and Asp$^{3.49(138)}$. However, in this construct, Arg$^{3.50(139)}$ is also significantly oriented toward Ala$^{3.54(143)}$ (12.7%), where it would be solvated in the aqueous cytoplasm.

ing of the Arg side chain.

Computational simulations provided structural hypotheses for the phenotypes observed with mutagenesis experiments. When studied mutants display detectable binding and affinities for GnRH similar to that of the wild-type receptor, we assume that the overall structure of the receptor was not perturbed significantly by these mutations. Mutant receptors without detectable binding also did not show detectable GnRH-induced signal transduction, suggesting that either the folding or the intracellular processing of these receptors was disrupted. The role of all potential Arg-cage side chains studied will be discussed separately based on the results from the computational simulations and the measured properties of the mutant constructs.

TABLE III

Binding and activation of wild-type and mutant GnRH receptors expressed in COS-1 cells

The K_i and B_{max} values are obtained from competition binding assays (mean ± S.E. from 3–5 experiments). The E_{max} and EC_{50} values are obtained from the phosphatidylinositol hydrolysis experiments (mean ± S.E. from 3–5 experiments). Basal activity was unchanged for all constructs. The mutations of Asp$^{3.49(138)}$ and Arg$^{3.50(139)}$ were generated in the mouse (m) GnRH receptor, whereas the mutations of Ile$^{3.54(143)}$ and Ile$^{3.46(135)}$ were made in the human (h) GnRH receptor. u, undetectable.

Constructs	Competition binding		Phosphatidylinositol assay		Relative receptor efficiency
	B_{max}	K_i GnRH	E_{max}	EC_{50}	
	%wt	*nM*	*%wt*	*nM*	
h wild type	100	1.4 ± 0.2	100	0.3 ± 0.1	1
Ile$^{3.54(143)}$Ala	109 ± 9	6.8 ± 1.5	69 ± 10	9.5 ± 1.3	0.2
Ile$^{3.54(143)}$Leu	25 ± 4	3.5 ± 1.8	66 ± 10	0.8 ± 0.3	2.5
Ile$^{3.54(143)}$Val	64 ± 8	1.9 ± 1.2	70 ± 7	0.3 ± 0.1	1.4
Ile$^{3.46(135)}$Ala	u	u	u	u	
Ile$^{3.46(135)}$Leu	13 ± 1	3.2 ± 1.5	96 ± 22	1.2 ± 0.1	4.8
Ile$^{3.46(135)}$Val	u	u	u	u	
m wild type	100	1.1 ± 0.4	100	0.4 ± 0.2	1
Asp$^{3.49(138)}$Ala	u	u	u	u	
Asp$^{3.49(138)}$Asn	56 ± 5	1.4 ± 0.4	98 ± 6	0.3 ± 0.1	2.9
Arg$^{3.50(139)}$His	u	u	u	u	
Arg$^{3.50(139)}$Lys	u	u	u	u	
Arg$^{3.50(139)}$Gln	559 ± 112	8.9 ± 1.0	68 ± 7	65.2 ± 7.0	0.04

Asp$^{3.49(138)}$—Computational experiments indicate that the propensity to form an ionic bond between Arg$^{3.50(139)}$ and Asp$^{3.49(138)}$ constrains the orientation of the Arg side chain. This constraint is relieved when the simulations are carried out for the Asp$^{3.49(138)}$ → Asn mutant or for a protonated Asp$^{3.49(138)}$. The results of mutagenesis in the GnRH receptor and in other receptors suggest that the interaction between Arg$^{3.50}$ and Asp$^{3.49}$ stabilizes the inactive receptor state. In the

α-adrenergic receptor, the mutation $Asp^{3.49} \rightarrow Asn$ leads to constitutive activation of the receptor (21, 35). We find that mutation of $Asp^{3.49} \rightarrow Asn$ leads to a modest increase in the efficiency of GnRH receptor activation similar to the reported result of the $Glu^{3.49} \rightarrow Gln$ mutation in rhodopsin (33).

In rhodopsin, receptor activation is accompanied by the uptake of two protons at cytoplasmic sites (32). One site of uptake has been identified as $Glu^{3.49}$, based on the lack of proton uptake by the $Glu^{3.49} \rightarrow Gln$ mutant (32). Thus neutralization of the 3.49 locus by either protonation or mutation favors the activated form of the receptor. To rationalize these results in the structural context of the proposed $Arg^{3.50}$-$Asp^{3.49}$ interaction, we performed the relevant computational experiment of protonating $Asp^{3.49(138)}$ in the GnRH receptor. In the Monte Carlo simulations, neutralization of the acidic group at position 3.49 either abolished ($Asp^{3.49} \rightarrow Asp$) or dramatically decreased ($Asp^{3.49} \rightarrow Asp\text{-}H$) the orientation of the Arg side chain toward the 3.49 locus (Table I). Based on these experimental and computational findings, we hypothesize that the conserved Arg side chain is held by $Asp^{3.49(138)}$ through an ionic bond in the inactive state of the receptor and that receptor activation involves the release of this constraint on the $Arg^{3.50(139)}$ side chain conformation, most likely by protonation of $Asp^{3.49}$.

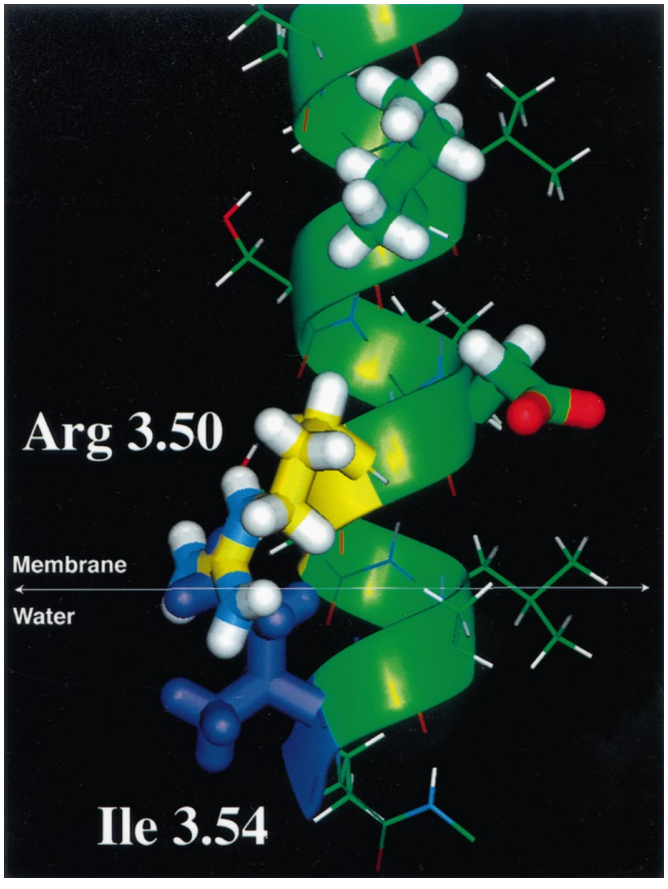

FIG. 6. **Proposed role of $I^{3.54(143)}$ in caging $Arg^{3.50(139)}$ through a steric clash.** Three-dimensional model of TMD 3 of the GnRH receptor where $R^{3.50(139)}$ attempts to adopt the (t, g−, t, g+) rotamer configuration oriented toward the C terminus or cytoplasmic boundary of TMD 3 but clashes with $Ile^{3.54(143)}$. Note that in this conformation $Arg^{3.50(139)}$ reaches the membrane-cytoplasm interface (*white line*), as determined for rhodopsin (25), and could thus become solvated.

$Ile^{3.54(143)}$—This locus shows a 100% conservation profile as a β-branched, bulky hydrophobic residue (Ile or Val). Experimentally, the $Ile^{3.54(143)} \rightarrow Val$ and the $Ile^{3.54(143)} \rightarrow Leu$ mutants were similar or more efficient than the wild-type receptor. The $Ile^{3.54(143)} \rightarrow Ala$ mutant was inefficient in mediating signal transduction and displayed a much lower receptor efficiency than the wild-type receptor. In simulations, the preferred orientations of the Arg side chain in the $Ile^{3.54(143)} \rightarrow Val$ and the $Ile^{3.54(143)} \rightarrow Leu$ mutants were similar to those observed in the wild-type receptor. However, in the $Ile^{3.54(143)} \rightarrow Ala$ mutant, a new orientation of the Arg side chain was significantly populated (14.3%, Table II). Analysis of the new rotamer conformations that are populated after mutation of $Ile^{3.54(143)} \rightarrow Ala$ provides a rationale for the observed phenotype. The bulky side chain of an Ile, Leu, or Val residue at this position would clash with the Arg side chain when this adopts the rotamer (t, g−, t, g+), as shown in Fig. 6. In contrast, an Ala at this position lacking the bulky side chain would allow this unfavorable conformation of the Arg residue, as can be seen in Fig. 5. According to the membrane-water boundary determined experimentally for rhodopsin and located between residues 3.52 and 3.53, the (t, g−, t, g+) rotamer of the Arg would orient the charged guanidinium group toward the aqueous cytoplasm. The strong solvation of the charged Arg side chain would inhibit it from further participation in any intramolecular interactions. Consequently, the results suggest that the structural role of $Ile^{3.54}$ is to restrict the positioning of $Arg^{3.50}$ during receptor activation. In the absence of a bulky side chain at this position, the solvation of $Arg^{3.50}$ in the cytoplasm may prevent it from forming the interactions most conducive to establishing an active receptor state.

$Ile^{3.46(135)}$—In the simulations, the wild-type receptor and $Ile^{3.46(135)}$ mutant constructs showed similar orientations of the Arg side chain and the surrounding residues. Mutagenesis experiments show that mutation of $Ile^{3.46(135)}$ to either Ala or Val is not tolerated, whereas substitution by Leu shows increased receptor efficiency as compared with the wild-type receptor. Both the lack of a local helix 3 effect of mutation of this locus in computational experiments and the highly restricted pattern of functionally tolerated mutations suggest

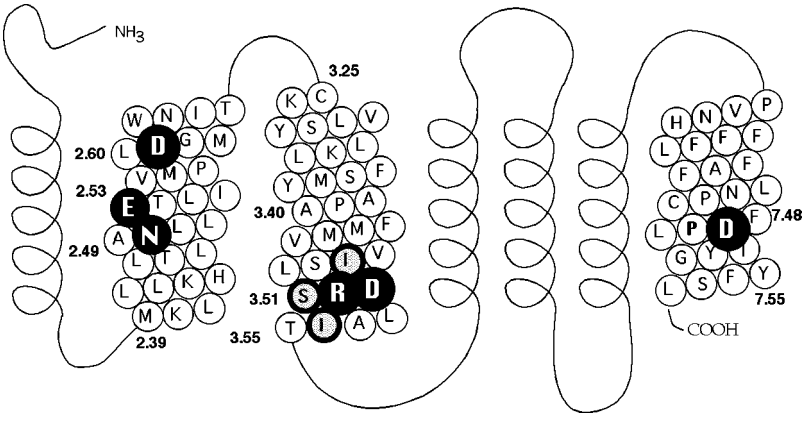

FIG. 7. **Schematic representation of the human GnRH receptor showing the position of Asp or Glu residues within the TMD (*black circles*), relative to $Arg^{3.50}$ (*black circle*) and the Arg-cage residues studied (*shaded*).** Modeling in three dimensions indicates that $Arg^{3.50}$ cannot interact with $Asp^{2.61}$ or $Glu^{2.53}$ in TMD 2, based on inferences from an engineered zinc-binding site between TMD 2 and TMD 3 (positions 2.64 and 3.28) (34). Aspartic acids $Asp^{3.49}$ and $Asp^{7.49}$ are in position to interact with $Arg^{3.50}$. $Asn^{2.50}$ is emphasized because it is a conserved Asp residue in most GPCRs and is proposed to interact with $Arg^{3.50}$ when $Asp^{7.49}$ is replaced by an Asn in these receptors.

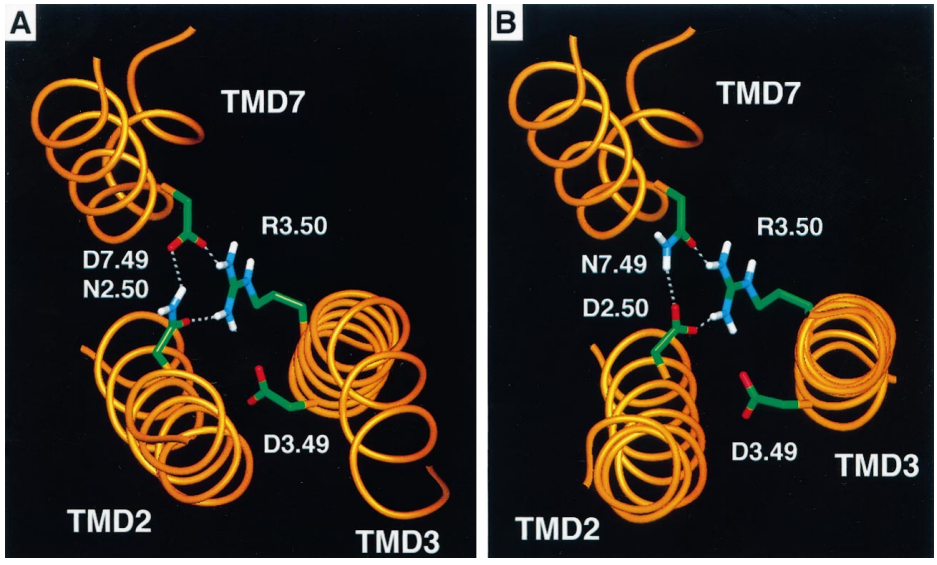

FIG. 8. **Three-dimensional model of TMDs 2, 3, and 7 of the GnRH receptor showing proposed interactions between $Arg^{3.50(139)}$ and the residues at positions 3.49–2.50–7.49.** *A*, GnRH receptor. $Arg^{3.50}$ interacts with $Asp^{3.49}$ and the side chains of $Asp^{7.49}$ and $Asn^{2.50}$. *B*, 5-HT_{2A} receptor. $Arg^{3.50}$ interacts with $Asp^{3.49}$ and the carbonyls of $Asn^{7.49}$ and $Asp^{2.50}$. Note that the set of interactions between the Arg residue and the TMD 2-TMD 7 loci in the GnRH receptor can be mimicked in the 5-HT2A receptor, despite the reciprocal arrangement of Asn and Asp at the 2.50 and 7.49 loci.

that $Ile^{3.46(135)}$ does not form a part of the Arg-cage motif and may have a role in interhelical interactions not considered in this study.

$Ser^{3.51(140)}$—Although there is a possible H-bonding interaction between $Arg^{3.50(139)}$ and $Ser^{3.51(140)}$, the interaction energy is not competitive with the strong $Arg^{3.50(139)}$-$Asp^{3.49(138)}$ interaction that predominates in the wild-type receptor. Removal of the H-bonding group of $Ser^{3.51(140)}$ by substitution to Ala produced no detectable alteration of the functional properties of the GnRH receptor (32), suggesting that $Arg^{3.50(139)}$ does not interact with this site or that the energetic contribution of such an interaction to the receptor activation mechanism is not significant.

Mechanistic Hypothesis for the Transition from an Inactive to an Active State of the Receptor—The implications of the pattern of interactions (*e.g.* $Arg^{3.50(139)}$-$Asp^{3.49(138)}$) and preferred conformations of the $Arg^{3.50(139)}$ side chain derived from conformational analysis on TMD 3 alone were further analyzed in the context of a seven TMD model of the receptor. Because the strongest interaction of $Arg^{3.50}$ is an ionic bond, we explored whether an alternative charge counterpart (Asp/Glu) could be found within other TMDs. The Asp or Glu residues present within the transmembrane domains of the GnRH receptor are shown schematically in Fig. 7. An acidic counterpart for the Arg would be expected to share its high degree of conservation and to reside at the cytoplasmic side of a TMD. However, the only conserved acidic group in the TMDs of the GnRH receptor is the $Asp^{3.49(138)}$ in the TMD 3 studied here. There are three nonconserved acidic residues present in the TMDs of the GnRH receptor at positions $Glu^{2.53(90)}$ and $Asp^{2.61(98)}$ in TMD 2 and $Asp^{7.49(319)}$ in TMD 7 (Fig. 7). An interaction of $Arg^{3.50(139)}$ with $Glu^{2.53(90)}$ or $Asp^{2.61(98)}$ is inconsistent with the geometrical constraints of an engineered Zn^{2+} binding site reported recently between TMD 2 and TMD 3 for the NK-1 receptor (36). Therefore these interaction possibilities were excluded. An interaction of $Arg^{3.50(139)}$ with the nonconserved $Asp^{7.49(319)}$ is possible in the complete model of the transmembrane portion of the GnRH receptor.

Notably, $Asp^{7.49(319)}$ forms part of a pair of conserved residues for which modeling and double mutant studies suggest an involvement in GPCR activation (8, 9). An unusual feature of the GnRH receptor is the presence of an Asn at position 2.50 in TMD 2 (Fig. 7) where nearly all other rhodopsin family GPCRs have an Asp. On the other hand, $Asp^{7.49(319)}$ in the GnRH receptor is an Asn in most GPCRs. This apparent interchange of conserved residues suggests that these residues may interact, a hypothesis supported by molecular modeling and double mutation studies of both the GnRH receptor (9) and the serotonin 5-HT_{2A} receptor (8). These results imply that $Asp^{7.49(319)}$ in the GnRH receptor substitutes functionally for the conserved Asp normally found at the 2.50 locus in other GPCRs and is therefore a suitable charged counterpart for $Arg^{3.50}$ in terms of their high conservation profile. We suggest that one function of $Asp^{7.49}$ in the GnRH receptor is to interact with $Arg^{3.50}$ in the active state of the receptor. Exploring this possibility in the context of a model of the GnRH receptor supports an interchangeable role of $Asp^{7.49(319)}$ and $Asn^{2.50(87)}$ in the interaction with the Arg residue in TMD 3, as shown in Fig. 8*A*. The Arg side chain is capable of extending from TMD 3 toward TMD 2 and TMD 7, where it can interact simultaneously with $Asp^{7.49(319)}$ and $Asn^{2.50(87)}$. We hypothesize that during receptor activation, $Asp^{3.49}$ becomes protonated, and $Asp^{7.49}$ substitutes for $Asp^{3.49}$ in forming an ionic interaction with $Arg^{3.50}$.

In most GPCRs, the active state interaction would occur with the $Arg^{3.50}$-$Asp^{2.50}$ bond as shown in Fig. 8*B*. Several models of GPCRs have proposed an interaction of $Arg^{3.50}$ with the $Asp^{2.50}$-$Asn^{7.49}$ locus (33, 20) but associate this interaction with the inactive state of the receptor. However, our data and results from other GPCRs described below support the role of this interaction with the conserved Asp/Asn pair at the 2.50–7.49 loci in stabilizing the active, not the inactive, receptor conformation. Thus, such a hypothesis is consistent with the finding in many GPCRs that mutations eliminating the charged character of $Asp^{2.50}$, which would be expected to destabilize the proposed active-state Arg-Asp interaction, either abolish or significantly decrease receptor activity (37). Furthermore, spectroscopic experiments in rhodopsin showing that $Asp^{2.50}$ is more strongly H-bonded upon activation (38), are also consistent with the proposed interaction between $Arg^{3.50}$ and $Asp^{2.50}$ in the active state.

In summary, the experimental and computational results suggest that the orientation of the highly conserved $Arg^{3.50(139)}$ side chain is constrained in the inactive receptor state by an ionic interaction with the neighboring conserved residue $Asp^{3.49(138)}$. During activation, $Asp^{3.49}$ becomes protonated, and the Arg side chain is released. The conserved bulky side chain of $Ile^{3.54(143)}$ modulates the positioning of the Arg side chain by keeping it away from the cytoplasmic aqueous medium and thereby promotes the interaction with $Asp^{7.49}$ ($Asp^{2.50}$ in other GPCRs) that characterizes the active state of the receptor. Further studies of other structural motifs that have the role of functional microdomains will allow refinement of these proposed molecular events underlying receptor activation.

Acknowledgment—We thank Dr. Colleen Flanagan for critical reading of the manuscript.

REFERENCES

1. Tsutsumi, M., Zhou, W., Millar, R. P., Mellon, P. L., Roberts, J. L., Flanagan, C. A., Dong, K., Gillo, B. & Sealfon, S. C. (1992) *Mol. Endocrinol.* **6,** 1163–1169
2. Chi, L., Zhou, W., Prikhozhan, A., Flanagan, C., Davidson, J. S., Golembo, M., Illing, N., Millar, R. P. & Sealfon, S. C. (1993) *Mol. Cell. Endocrinol.* **91,** 1–6
3. Gudermann, T., Schoneberg, T. & Schultz, G. (1997) *Annu. Rev. Neurosci.* **20,** 399–427
4. Farrens, D. L., Altenbach, C., Yang, K., Hubbell, W. L. & Khorana, H. G. (1996) *Science* **274,** 768–770
5. Sheikh, S. P., Zvyaga, T. A., Lichtarge, O., Sakmar, T. P. & Bourne, H. R. (1996) *Nature* **383,** 347–350
6. Javitch, J. A., Fu, D., Liapakis, G. & Chen, J. (1997) *J. Biol. Chem.* **272,** 18546–18549
7. Probst, W. C., Snyder, L. A., Schuster, D. I., Brosius, J. & Sealfon, S. C. (1992) *DNA Cell Biol.* **11,** 1–20
8. Sealfon, S. C., Chi, L., Ebersole, B. J., Rodic, V., Zhang, D., Ballesteros, J. A. & Weinstein, H. (1995) *J. Biol. Chem.* **270,** 16683–16688
9. Zhou, W., Flanagan, C., Ballesteros, J. A., Konvicka, K., Davidson, J. S., Weinstein, H., Millar, R. P. & Sealfon, S. C. (1994) *Mol. Pharmacol.* **45,** 165–170
10. Schertler, G. F., Villa, C. & Henderson, R. (1993) *Nature* **362,** 770–772
11. Schertler, G. F. & Hargrave, P. A. (1995) *Proc. Natl. Acad. Sci. U. S. A.* **92,** 11578–11582
12. Baldwin, J. M. (1994) *Curr. Opin. Cell Biol.* **6,** 180–190
13. Sealfon, S. C., Zhou, W., Almaula, N. & Rodic, V. (1996) *Methods Neurosci.* **29,** 143–196
14. Ballesteros, J. A. & Weinstein, H. (1995) *Methods Neurosci.* **25,** 366–428
15. Laakkonen, L. J., Guarnieri, F., Perlman, J. H., Gershengorn, M. C. & Osman, R. (1996) *Biochemistry* **35,** 7651–7663
16. Almaula, N., Ebersole, B. J., Ballesteros, J. A., Weinstein, H. & Sealfon, S. C. (1996) *Mol. Pharmacol.* **50,** 34–42
17. Zhang, D. & Weinstein, H. (1993) *J. Med. Chem.* **36,** 934–938
18. Scheer, A. & Cotecchia, S. (1997) *J. Recept. Signal Transduct. Res.* **17,** 57–73
19. Almaula, N., Ebersole, B. J., Zhang, D., Weinstein, H. & Sealfon, S. C. (1996) *J. Biol. Chem.* **271,** 14672–14675
20. Min, K. C., Zvyaga, T. A., Cypess, A. M. & Sakmar, T. P. (1993) *J. Biol. Chem.* **268,** 9400–9404
21. Scheer, A., Fanelli, F., Costa, T., De Benedetti, P. G. & Cotecchia, S. (1996) *EMBO J.* **15,** 3566–3578
22. Oliveira, L., Paiva, A. C. M., Sander, C. & Vriend, G. (1994) *Trends Biochem. Sci.* **15,** 170–172
23. Honda, Z., Nakamura, M., Miki, I., Minami, M., Watanabe, T., Seyama, Y., Okado, H., Toh, H., Ito, K., Miyamoto, T. & Shimizu, T. (1991) *Nature* **349,** 342–346
24. Javitch, J. A., Fu, D., Chen, J. & Karlin, A. (1995) *Neuron* **14,** 825–831
25. Farahbakhsh, Z. T., Ridge, K. D., Khorana, H. G. & Hubbell, W. L. (1995) *Biochemistry* **34,** 8812–8819
26. Rees, D. C., Komiya, H., Yeates, T. O., Allen, J. P. & Feher, G. (1989) *Annu. Rev. Biochem.* **58,** 607–633
27. Zhou, W., Rodic, V., Kitanovic, S., Flanagan, C. A., Chi, L., Weinstein, H., Maayani, S., Millar, R. P. & Sealfon, S. C. (1995) *J. Biol. Chem.* **270,** 18853–18857
28. Lowry, O. H., Rosebrough, N. J., Farr, A. L. & Randall, R. J. (1951) *J. Biol. Chem.* **193,** 265–275
29. Munson, P. J. & Rodbard, D. (1980) *Anal. Biochem.* **107,** 220–239
30. McGregor, M. J., Islam, S. A. & Sternberg, M. J. (1987) *J. Mol. Biol.* **198,** 295–310
31. Gray, T. M. & Matthews, B. W. (1984) *J. Mol. Biol.* **175,** 75–81
32. Arnis, S., Fahmy, K., Hofmann, K. P. & Sakmar, T. P. (1994) *J. Biol. Chem.* **269,** 23879–23881
33. Cohen, G. B., Yang, T., Robinson, P. R. & Oprian, D. D. (1993) *Biochemistry* **32,** 6111–6115
34. Arora, K. K., Cheng, Z. & Catt, K. J. (1997) *Mol. Endocrinol.* **11,** 1203–1212
35. Scheer, A., Fanelli, F., Costa, T., De Benedetti, P. G. & Cotecchia, S. (1997) *Proc. Natl. Acad. Sci. U. S. A.* **94,** 808–813
36. Elling, C. E. & Schwartz, T. W. (1996) *EMBO J.* **15,** 6213–6219
37. van Rhee, A. M. & Jacobson, K. A. (1996) *Drug Dev. Res.* **37,** 1–38
38. Rath, P., DeCaluwe, L. L., Bovee-Geurts, P. H., DeGrip, W. J. & Rothschild, K. J. (1993) *Biochemistry* **32,** 10277–10282

Functional Microdomains in G-protein-coupled Receptors: THE CONSERVED ARGININE-CAGE MOTIF IN THE GONADOTROPIN-RELEASING HORMONE RECEPTOR

Juan Ballesteros, Smiljka Kitanovic, Frank Guarnieri, Peter Davies, Bernard J. Fromme, Karel Konvicka, Ling Chi, Robert P. Millar, James S. Davidson, Harel Weinstein and Stuart C. Sealfon

J. Biol. Chem. 1998, 273:10445-10453.
doi: 10.1074/jbc.273.17.10445
